Article:
Shu, YD, Liu, JJ, Zhang, Y et al. (1 more author) (2019) A multi-stage multi-component transfer rate morphological population balance model for crystallization processes. CrystEngComm, 21 (28). pp. 4212-4220. ISSN 1466-8033

https://doi.org/10.1039/C9CE00438F

Multi-stage Multi-component Transfer Rate Morphological Population Balance Model for Crystallisation Processes

Yi D. Shu[a], Jing J. Liu[a] Yang Zhang[a], and Xue Z. Wang[b,a,*]

[a]School of Chemistry and Chemical Engineering, South China University of Technology，Guangzhou, Guangdong 510640, China

[b]School of Chemical and Process Engineering, University of Leeds, Leeds LS2 9JT, U.K.

[*]Correspondence author:

Professor Xue Z. Wang

Personal Chair in Intelligent Measurement and Control

School of Chemical and Process Engineering, University of Leeds

Leeds LS2 9JT, UK

Tel +44 113 343 2427, Fax +44 113 343 2384

Email:x.z.wang@leeds.ac.uk

&

School of Chemistry and Chemical Engineering,

South China University of Technology

381 Wushan Rd, Tianhe District, Guangzhou, PR China 510641

Tel: +86 20 8711 4000, Fax: +86 20 8711 4000

Email: xuezhongwang@scut.edu.cn

Abstract

A model was proposed for single crystals for modeling the non-equilibrium crystal growth (CrystEngComm, 2018, **20**, 5143-5153)**.** It describes mathematically and digitally the non-equilibrium growth behavior of single crystals using multi-component transfer rate models, as well as considering multi-component phase equilibria, adsorption, orientation and crystallization of individual molecules on crystal faces. In this paper, the model for single crystal growth is extended to modeling a population of crystals in a crystalliser by incorporating it into morphological population balance equations. The resulting modeling approach, i.e. the multi-stage multi-component transfer rate morphological population balance models (M^3PBEs) model is able to predict the spatial and temporal distribution of multi-components inside crystals during the course of crystallisation as well as the multi- component composition in the product crystals. The new modeling approach is introduced by reference to a case study of $NaNO_3$ batch cooling crystallization in water.

Keywords: Morphological Population Balance model; multi-component mass transfer; non-equilibrium; crystal shape; crystal composition

Nomenclature

Subscript

i	Component number
j	Moment number
k	Face number

Variable and Parameter

A_k	Area of face k, m^2
C	Total number of components
F	Total number of faces
G_k	Facet growth rate, m/s
H_i	Component mole fraction change rate, s^{-1}
$K_{i,k}$	Langmuir constant of adsorption
$K^r_{i,k}$	Equilibrium ratio of component mole fraction (adsorption layer to solid)
$k^d_{i,k}$	liquid phase mass transfer coefficient, $mol/(m^2s)$
$k^r_{i,k}$	mass transfer coefficient from adsorbed solute to crystallized solute, $mol/(m^2s)$
$l_{i,j,k}$	Component mole fraction in solution, mol
M_i	Mole weight, kg/mol
$M^I_{i,j,k}$	Mass balance equation of interface
$M^L_{i,j}$	Mass balance equation of liquid
$M^S_{i,j,k}$	Mass balance equation of solid
$N^L_{i,j,k}$	Mass transfer rate in liquid,
p	Order of solid mass transfer rate equation
$Q^{ads}_{i,j,k}$	Adsorption equilibrium equation
$Q^S_{i,j,k}$	Solid phase and
$R^L_{i,j,k}$	Liquid phase mass transfer equation
$R^S_{i,j,k}$	Solid phase mass transfer equation
$S^{ads}_{j,k}$	Summation relation of mole fractions in adsorption layer
$S^L_{j,k}$	Summation relation of mole fractions in liquid
$s_{i,j,k}$	Component mole number in the crystal
t	Time, s
V	Crystal volume, m^3
X	Vector of facet normal distances
x_k	Facet normal distance from the crystal center
$x^I_{i,j,k}$	Liquid component molar fraction on the interface
$x^L_{i,j}$	Component molar fraction in the solution bulk
Y	Vector of component mole fractions
y_i	Component mole fraction in the crystal
$y^I_{i,j,k}$	Solid component molar fraction on the interface
$y^S_{i,j,k}$	Component molar fraction in the formed crystal layer
$z_{i,j,k}$	Component molar fraction in the adsorption layer
Ψ	Crystal population number density,

	mol/s		#/m^F, F is the number of independent faces
$N^S_{i,j,k}$	Mass transfer rate in solid, mol/s	ρ_i	Component density, kg/m^3

Introduction

Crystallization is a chemical engineering separation process widely used for product purification. During crystallization, the so-called impurities are mainly left in the solution, while the product component such as a drug active pharmaceutical ingredient (API) is purified. Since a crystal is a well-structured solid particle with multiple faces, each being selective in adsorbing and crystallizing individual components, one could imagine that inside each crystal, in each face direction, at any size dimensional location, the composition of the multi-components would vary. In a recent study [1] a modeling technique for single crystals was proposed that allows the spatial distribution of multiple compounds inside the crystal to be estimated any time during crystallization. In addition, the facet growth rate in the model was not related directly to supersaturation or impurities like the models used by previous researchers such as Kubota [2]. Instead, it depends on the amount of materials transferred, adsorbed or crystallized onto the crystal faces and the material density. As a result, the solid-liquid phase equilibrium assumption Borsos et al.[3] is unnecessary because inclusion of impurities and the evolution of crystal composition can be directly calculated. Simultaneous prediction of both composition and shape of a crystal can be achieved.

The new modeling method proposed by authors [1] only achieved simulation for single crystals. In this paper, the method is extended to a crystal population in a stirred crystallizer. This was achieved by incorporating it into morphological population balance equations[4]. The new modeling technique is called multi-stage multi-component transfer rate morphological population balance equations (M^3PBE). The remaining of this article is organized as follows. Firstly, a brief introduction of the multi-component mass transfer rate based model for single crystals will be given.

Then the integration into morphological population balance equation will be described. Afterwards the M^{3}PBE model will be applied to simulate the composition, shape and size distribution of $NaNO_3$ crystal population in the presence of KNO_3 impurities. And finally conclusions will be drawn.

Brief Introduction to Single Crystal Model

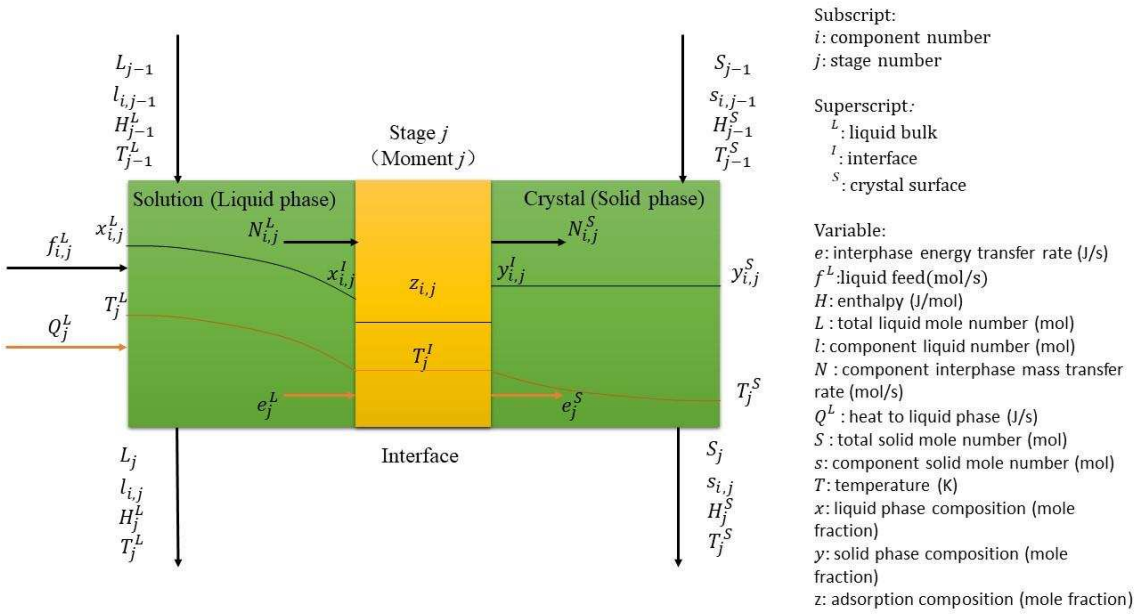

Fig. 1 Schematic diagram of non-equilibrium stage model of a single crystal on a face.

Fig. 1 depicts the interface model between one face k (k = 1…F) of a crystal, and the liquid phase at time j. Let's examine the kinetic and thermodynamic phenomena involved for a component i that initially in the body liquid phase to crystallize on this crystal phase k. It can be considered as involving three steps. First, component i diffuses (or mass transfers) from the solution bulk to the interface, as a result of the driving force, i.e. concentration difference between the bulk solution and the interface, x_i^L-x_i^I. Here it is assumed that the bulk solution is well mixed so the composition of i in the bulk solution is uniform. Secondly, between the liquid phase and the solid phase there is an interface layer. Suppose the interface is so thin that there is no mass transfer resistance and the layer is homogeneous and we denote the composition of i component in it as z_i. In addition, it is assumed that the interface layer is formed by

component adsorption, and the adsorption is fast that x_i^I and z_i can be assumed in adsorption equilibrium. In this paper the adsorption equilibrium is modeled with Langmuir adsorption isotherms. Thirdly, the adsorbed component i is integrated onto the crystal face. In here, the diffusion of component i in the solid phase is neglected. In the solid phase it is modeled like a "reaction" process that the adsorbed solute molecule i is included into the crystal. The driving force of this step is the difference between the adsorption molar fraction ($z_{i,k}$) and the equilibrium molar fraction that depends on the solid interface molar fraction ($y^I_{i,k}$). Here k is the k^{th} face of the crystal, k= 1,2,...,F. Therefore, for component i, on face k， the interface model equations are as follows,

$$R^L_{i,j,k} \equiv N^L_{i,j,k} - k^d_{i,k} A_k (x^L_{i,j} - x^I_{i,j,k}) = 0 \tag{1}$$

$$Q^{ads}_{i,j,k} \equiv z_{i,j,k} - \frac{K_{i,k} x^I_{i,j,k}}{1 + \sum_{m=1}^{C-1} K_{m,k} x^I_{m,j,k}} = 0 \tag{2}$$

$$R^S_{i,j,k} \equiv N^S_{i,j,k} - k^r_{i,k} A_k (z_{i,j,k} - K^r_{i,k} y^I_{i,j,k})^p = 0 \tag{3}$$

$R^L_{i,j,k}$, $Q^{ads}_{i,j,k}$ and $R^S_{i,j,k}$ represent the liquid phase mass transfer, adsorption equilibrium and solid phase mass transfer equations of component i, on face k, at moment j respectively; $k^d_{i,j,k}$ is the liquid phase mass transfer coefficient in mol/(m^2s), where the superscript d denotes that the mass transfer coefficient is due to molecular diffusion. $k^r_{i,j,k}$ is the mass transfer coefficient from adsorbed solute to crystallized solute in mol/(m^2s),where superscript r denotes that the mass transfer coefficient $k^r_{i,j,k}$ equation is in the form of a kinetic expression. $K^r_{i,k}$ is the equilibrium ratio of component i on crystal face k. p is the order, $K_{i,k}$ is the simplified Langmuir constant of adsorption of component i on crystal face k. According to Karpiński's suggestion, assigning the reaction order p = 2 would be the most appropriate choice in light of the BCF (Burton, Cabrera and Frank) growth theory.[5]

The component molar fraction in the bulk liquid phase can be expressed as the

molar fractions of components in the liquid phase as:

$$x^{L}_{i,j,k} = \frac{l_{i,j,k}}{\sum_{n=1}^{C} l_{n,j,k}} \tag{4}$$

wherein $x^{L}_{i,j,k}$ is the molar fraction of component i in the solution at moment j on face k, $l_{i,j,k}$ is the mole number of component i in the solution at moment j on face k.

In this model, the diffusion in the solid phase is neglected. Therefore, the growth of crystal is assumed to be purely layer-by-layer stacking of crystallized material. Therefore, the solid composition related to the mass transfer is equal to the composition of the crystal layer that formed in the last moment (i =1,2,…,C).

$$Q^{S}_{i,j,k} \equiv y^{I}_{i,j,k} - y^{S}_{i,j,k} = 0 \tag{5}$$

And the component molar fractions in the crystal layer formed at moment j can be expressed by:

$$y^{S}_{i,j,k} = \frac{s_{i,j,k} - s_{i,j-1,k}}{\sum_{n=1}^{C} (s_{n,j,k} - s_{n,j-1,k})},\ j \geq 2 \tag{6}$$

wherein $s_{i,j,k}$ is the mole number of component i in the crystal at moment j on face k

The inclusion of these three steps are inspired by the work of Karpiński[5] and Martins and Rocha[6] on crystal growth of a single solute. The first and the third steps are described by corresponding rate equations that depend on the mass transfer driving force while the second step is assumed to follow the adsorption equilibrium.

With the interface model introduced above, it can now consider the temporal change of a crystal in the course of crystallization. If the process is divided into discretized moments, each moment can be regarded as a “stage” in the time space. Then the crystal growth in time can be described in the same way as the stage model of a distillation columns[7]. Fig. 1shows the details of a stage model. On the stage, j represents the jth moment, or the jth stage. The entering and leaving arrows represent the status of the solution and crystal at moment j-1 and j, or at stage j-1 and stage j. The state of a stage is described by a series of variables shown in Fig. 1, including

total moles of liquid and solid, L and S (mol), component moles of liquid and solid l and s (mol), enthalpy (J/mol), temperature (K). These variables are related to each other by equations. At the moment j, i.e. at stage j, mass and heat transfer takes place between the solution and the solid crystal face. The transfer rates of mass and heat are denoted as N (mol/s) and e (J/s). The superscripts L and S represent liquid and solid phases, and the subscripts i and j represent component i and stage j respectively. The model can also consider feeding (e.g. adding seeds) and heat exchange with the streams $f_{i,j}^{L}$ and Q_j^L. In this paper the focus is placed on crystal growth modeling so heat transfer is neglected. If there is no feeding after the crystallization begins, the mass balance equations for liquid phase, solid phase and interface can be written in turn as:

$$M_{i,j}^{L} \equiv l_{i,j} - l_{i,j-1} + \sum_{k=1}^{F} N_{i,j,k}^{L} \Delta t = 0 \tag{7}$$

$$M_{i,j,k}^{S} \equiv s_{i,j,k} - s_{i,j-1,k} + N_{i,j,k}^{S} \Delta t = 0 \tag{8}$$

$$M_{i,j,k}^{I} \equiv N_{i,j,k}^{L} \Delta t - N_{i,j,k}^{S} \Delta t = 0 \tag{9}$$

The summation of the compositions of components of either the liquid phase, or the solid phase, or for the adsorption phase should be 1. It is called the summation equation. The solid phase summation equations can be obtained from the summation of $Q^{S}_{i,j,k}$ so they are not independent equations and won't be listed here.

$$S_{j,k}^{L} \equiv \sum_{i=1}^{C} x_{i,j,k}^{I} - 1 = 0 \tag{10}$$

$$S_{j,k}^{ads} \equiv \sum_{i=1}^{C} z_{i,j,k} - 1 = 0 \tag{11}$$

There are $C+6CF$ unknown quantities for each stage j. These are the component liquid mole number ($l_{i,j}$: C in number), the solid mole number ($s_{i,j,k}$: CF), the liquid composition at the interface ($x^{I}_{i,j,k}$: CF), the solid composition at the interface ($y^{I}_{i,j,k}$: CF), the adsorption phase composition at the interface ($z_{i,j,k}$: CF), the mass transfer rate ($N^{L}_{i,j,k}$: CF and $N^{S}_{i,j,k}$: CF). The $C+6CF$ independent equations that permits these unknown quantities include: component material balances for the liquid ($M^{L}_{i,j}$: C in

number), component material balances for the solid ($M^{S}_{i,j,k}$: CF), component material balances around the interface ($M^{I}_{i,j,k}$: CF), the liquid phase mass transfer rate equations ($R^{L}_{i,j,k}$: (C-1)F), the solid phase mass transfer rate equations ($R^{S}_{i,j,k}$: CF), the interface solid component model ($Q^{S}_{i,j,k}$: CF), the interface adsorption equilibrium ($Q^{ads}_{i,j,k}$: (C-1)F), the summation equations ($S^{L}_{j,k}$: F and $S^{ads}_{j,k}$: F). If the component molar numbers of solution and crystal at the last moment are known and the mass transfer rate can be obtained, the component molar numbers of solution and crystal at the present moment can be calculated in accordance with mass balance. Therefore the number of equations is equal to the number of variables so the equations can be solved using an appropriate numerical solution algorithm. In our model, the "streams" between stages are not countercurrent but concurrent. Therefore our model can be solved stage by stage, which is more convenient than solving non-equilibrium stage models for a distillation column. By solving the equations, the component mass transfer rates to each of the crystal face can be obtained. Then a particular facet crystal growth rate can be calculated by summing up all the component mass transfer rates (in mol/s) to that face divided by the component densities and molar weights and the face area. The change of the crystal composition can also be calculated according to the component solid mole number.

The M^{3}PBE Model

After the non-equilibrium stage model for a single crystal is introduced above, the attention is turned to incorporating the model to Morphological Population Balance Equation. Population Balance Equation (PBE) is the most common method to model the size distribution of a crystal population. Ma et al. proposed Morphological Population Balance Equation (M-PBE) model to simulate the shape distribution or multi-dimensional size distribution of crystals.[4]

The compositions of components should be incorporated into the number population density distribution and then M-PBE can be extended to multi-stage multi-component transfer rate morphological population balance equations (M^{3}PBEs)

model as Eq. (12):

$$\frac{\partial \Psi(\mathbf{X},\mathbf{Y},t)}{\partial t}+\sum_{k=1}^{F}\frac{\partial}{\partial x_k}\left(G_k(\mathbf{X},\mathbf{Y})\Psi(\mathbf{X},\mathbf{Y},t)\right)+\sum_{i=1}^{C-1}\frac{\partial}{\partial y_i}\left(H_i(\mathbf{X},\mathbf{Y})\Psi(\mathbf{X},\mathbf{Y},t)\right)=0 \qquad (12)$$

wherein Ψ is the number population density function of crystal, $\mathbf{X}$ is the vector of normal distances from the crystal faces to the geometric center of a crystal with elements x_k (k=1,2,…,F). F is the number of crystal faces. $\mathbf{Y}$ is the vector of mole fraction of crystal components, with elements y_i (i=1,2,…,C-1). C is the number of chemical components. t is time. G_k is the facet growth rate of face k and H_i is the mole fraction change rate of component i.

One difference between the M^{3}PBEs and the previous morphological population balance equations is that the face growth rate is calculated with the mass transfer rates from the non-equilibrium stage model rather than the conventional growth rate kinetics equations, as Eq. (13) shows:

$$G_k(\mathbf{X},\mathbf{Y})=\frac{\sum_{i=1}^{C}\left[N_{i,k}(\mathbf{X},\mathbf{Y})M_i/\rho_i\right]}{A_k(\mathbf{X})} \qquad (13)$$

wherein $N_{i,k}$ is the mass transfer rate of component i on face k, in mol/s. M_i is the molar weight and ρ_i is the density of component i. $A_k(\mathbf{X})$ is the area of face k, which can be obtained according to the geometric information of the crystal. If k stands for a symmetric-related face group, A_k should be the sum of all the face areas in that group.

The mole fraction change rate of component i can also be calculated with the mass transfer rates as Eq. (14) shows:

$$H_i(\mathbf{X},\mathbf{Y})=\frac{1}{V(\mathbf{X})\sum_{i=1}^{C}(y_i\rho_i/M_i)}\left(\sum_{k=1}^{F}N_{i,k}(\mathbf{X},\mathbf{Y})-y_i\sum_{i=1}^{C}\sum_{k=1}^{F}N_{i,k}(\mathbf{X},\mathbf{Y})\right) \qquad (14)$$

wherein $V(\mathbf{X})$ is the crystal volume.

With the H and G specified, Eq. (10) can be numerically solved using the high resolution algorithm proposed by Gunawan, Fusman and Braatz[8].

In summary, the framework of our method is as Fig. 2 shows. For each discretized moment, we firstly solve the stage model according to the amount of each

component in the liquid and solid phase at that moment. Then we can get the mass transfer rate and calculate the facet growth rate and mole fraction change rate. Afterwards, the M^3PBE equation can be solved using the high resolution algorithm [8] and then the data of amount of each component in the liquid and solid phase at that moment can be updated and the calculation can be iterated moment by moment until the desired duration of crystallization processes is reached.

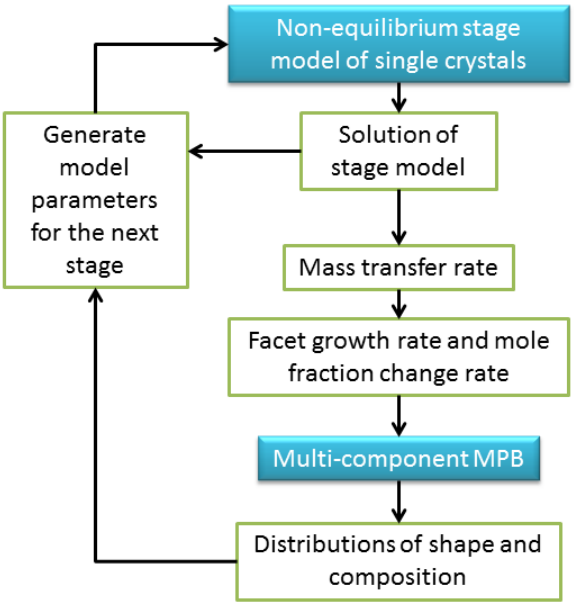

Fig. 2 Framework of method

Case study

Simulation scenario

In Shu's work[1], the single crystal model was applied to modelling a single $NaNO_3$ crystal growth from aqueous solution in the presence of impurity KNO_3. In the case study of this work we choose the same material but now it is for the whole crystal population in the crystallizer.

Fig. 3 is the equilibrium morphology of a $NaNO_3$ crystal which was predicted by

Benages-Vilau[9] and also observed by Wu et al.[10] As Fig. 3 shows, a $NaNO_3$ crystal is rhombohedral with six faces. These faces can be classified into three groups of crystallographically equivalent faces, i.e. two {104}, two $\{\bar{1}14\}$ and two $\{0\bar{1}4\}$. the values of α, β, and γ are 90.57°, 102.72°, and 102.72°. Wu et al. also measured the crystal face specific growth kinetics of all the three faces.

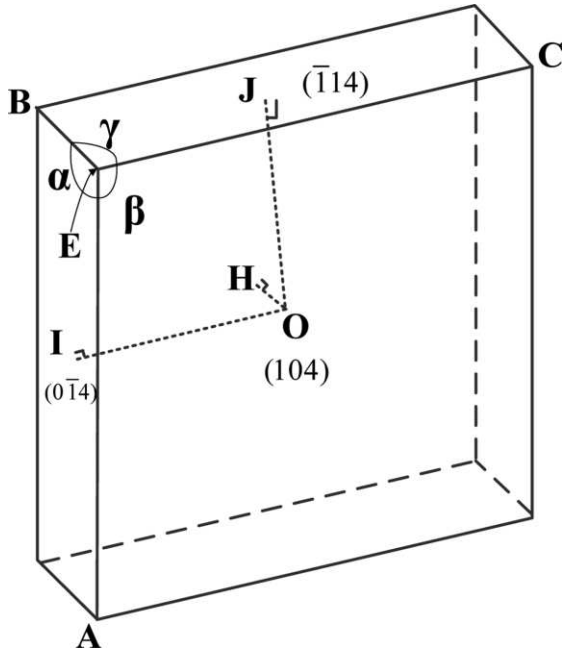

Fig. 3 Equilibrium and experimental morphology of a $NaNO_3$ crystal

Benages-Vilau et al. studied the morphology change of $NaNO_3$ from aqueous solution in the presence of K^+ or Li^+ ions. They found that the addition of these impurities led to a sudden decrease of the {104} face and caused the morphology change[11].

Initially 1000 pure $NaNO_3$ crystals are loaded in the crystallizer as crystal seeds and the crystallization temperature was kept at 25°C. KNO_3 was assumed to be adsorbed on {104} face only. The initial solution consists of 181.14g of $NaNO_3$, 0.21g of KNO_3 (the molar ratio of $NaNO_3/KNO_3$ is 1000) and 188.86g of H_2O. The initial distributions of face normal distances of {104}, $\{\bar{1}14\}$ and $\{0\bar{1}4\}$ are in Gaussian distribution as Eq. (15):

$$\Psi(\mathbf{X}, y, 0) = \frac{1}{(2\pi)^{3/2}\sigma_1\sigma_2\sigma_3} e^{-\frac{1}{2}\left[\left(\frac{x_1-\mu_1}{\sigma_1}\right)^2+\left(\frac{x_2-\mu_2}{\sigma_2}\right)^2+\left(\frac{x_3-\mu_3}{\sigma_3}\right)^2\right]} \quad (15)$$

wherein $\Psi(\mathbf{X}, y, 0)$ is the initial number density distribution function, x_1, x_2 and x_3 stand for the of face normal distances of {104}, $\{\bar{1}14\}$ and $\{0\bar{1}4\}$. μ_1, μ_2 and μ_3 are the mean values of corresponding face normal distances and σ_1, σ_2 and σ_3 are the standard deviations. Their values are 100 μm, 300 μm, 300 μm, 25 μm, 50 μm and 50 μm respectively. The initial distribution curves of the normal distances of {104}, $\{\bar{1}14\}$ and $\{0\bar{1}4\}$ are as Fig. 4 shows.

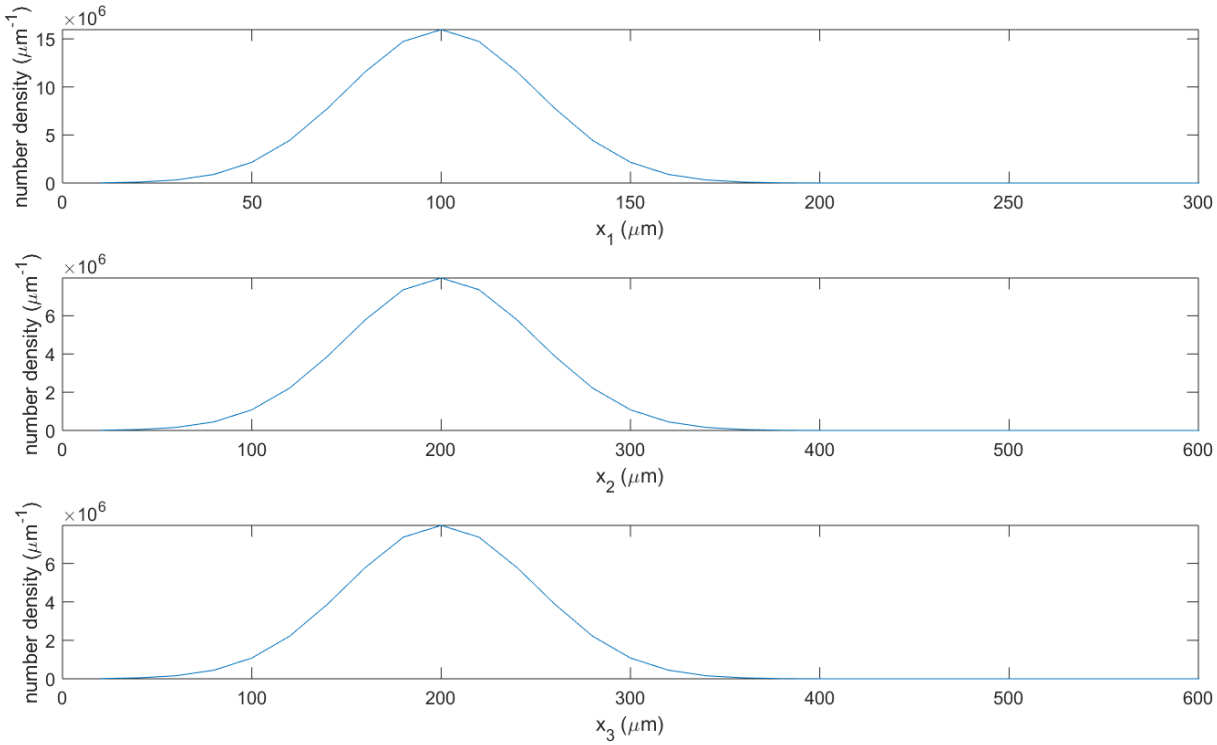

Fig. 4 Initial distribution of facet normal distances

Model parameters

In our previous work, we discussed the determination of parameter values of the model [1]. The liquid mass transfer coefficients can be calculated based on correlation equation given by Geankoplis [12] and the necessary property parameters of diffusivity, density and viscosity aqueous $NaNO_3$ and KNO_3 can be found in the work of Graber et al. [13]. Other parameters corresponding to $NaNO_3$ can be regressed according to the solubility data [14] [15], and the facet growth rate measurement given by Wu et al.[10]. Their

values are in Table 1.

Table 1 Model parameters corresponding to $NaNO_3$

Parameter	{104}	$\{\bar{1}14\}$	$\{0\bar{1}4\}$
$K_{i,k}$	77.68	109.32	114.78
$K^r_{i,k}$	0.927	0.947	0.950
$k^r_{i,k}(10^3 mol \cdot m^{-2} \cdot s^{-1})$	0.650	1.520	1.801

Because the measurement data of growth of $NaNO_3$ crystals in the presence of KNO_3 impurity are unavailable, the parameters corresponding to KNO_3 cannot be regressed. According to the experiment results of Benages-Vilau et al., the addition of KNO_3 impurity poisoned the {104} face growth rate[11]. Therefore, in our previous work, KNO_3 was assumed to affect the {104} face only and the parameters corresponding to other faces are assumed to be 0. The values of $K_{i,k}$, $K^r_{i,k}$ and $k^r_{i,k}$ for KNO_3 on face {104} are assumed to be 776.8, 0.9805 and 64.97 $mol \cdot m^{-2} \cdot s^{-1}$ respectively. The sensitivity of these parameters value were also discussed.[1] In the following simulation, we will use the same parameter values.

Simulation result

With M^3PBE, we can calculate the time-depended joint number density distribution of the three normal distances and the overall KNO_3 concentration of the crystals. Since it is hard to show a 4-dimensional distribution, we transformed the simulated distribution into three 2-dimenisonal joint distribution of one of the three normal distances and the overall KNO_3 concentration as Fig. 5 shows. All the crystals are initially pure so the initial distributions are 1-dimensional peaks. During the crystallization, KNO_3 goes into the crystals so the distributions change into 2-dimensional surfaces. As $NaNO_3$ is consumed, the growth rates decreases.

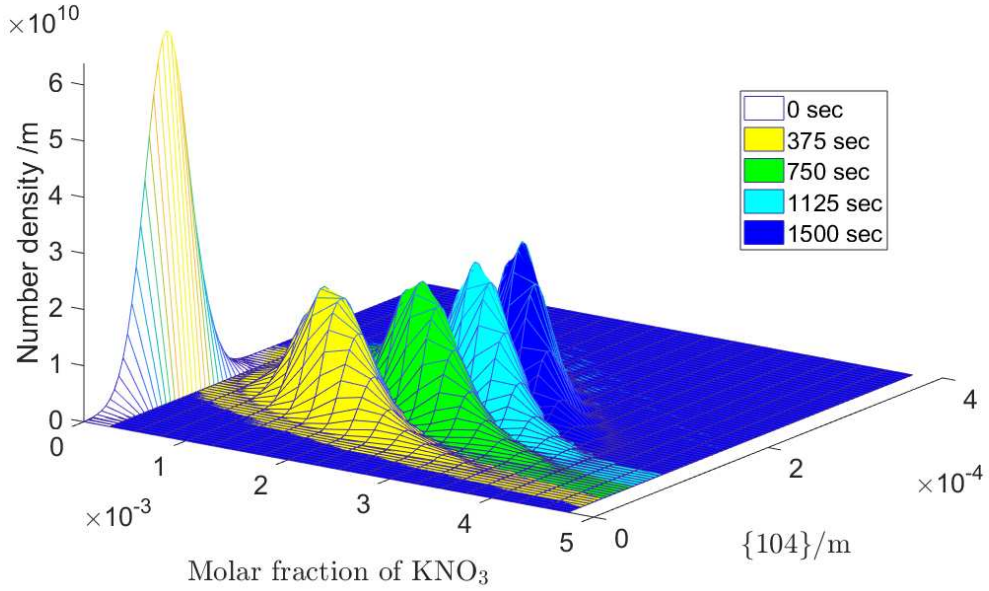
×10^10
Number density /m
0 sec
375 sec
750 sec
1125 sec
1500 sec
×10^-3
Molar fraction of KNO3
×10^-4
{104}/m

(a)

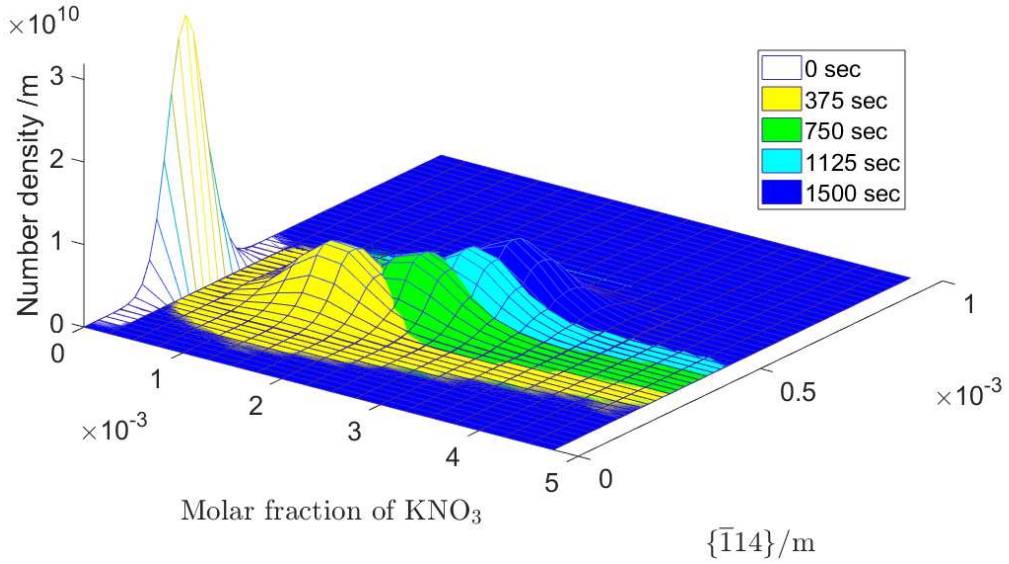
×10^10
Number density /m
0 sec
375 sec
750 sec
1125 sec
1500 sec
×10^-3
Molar fraction of KNO3
×10^-3
{1̄14}/m

(b)

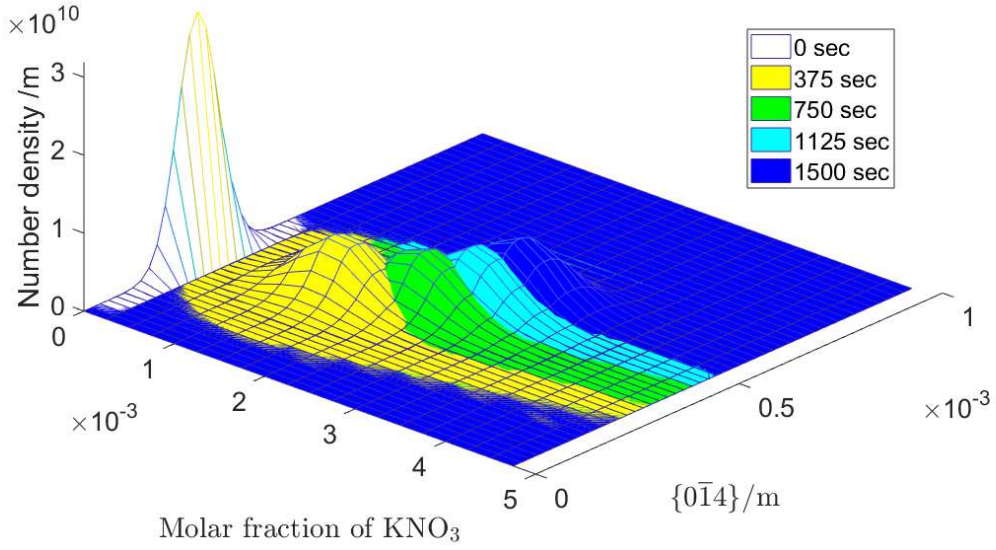

(c)

Fig. 5 Joint number density of crystal KNO_3 concentration and facet normal distance. (a) Facet normal distance of {104} and crystal KNO_3 concentration; (b) Facet normal distance of {$\bar{1}$14} and crystal KNO_3 concentration; (c) Facet normal distance of {0$\bar{1}$4} and crystal KNO3 concentration

The concentration distribution curves at different moments are shown in Fig. 6. It can be seen that the movement of the curve peak as crystallization goes on, which indicates the increasing rate of overall KNO_3 concentration in crystals, decreases because of the consumption of KNO_3.

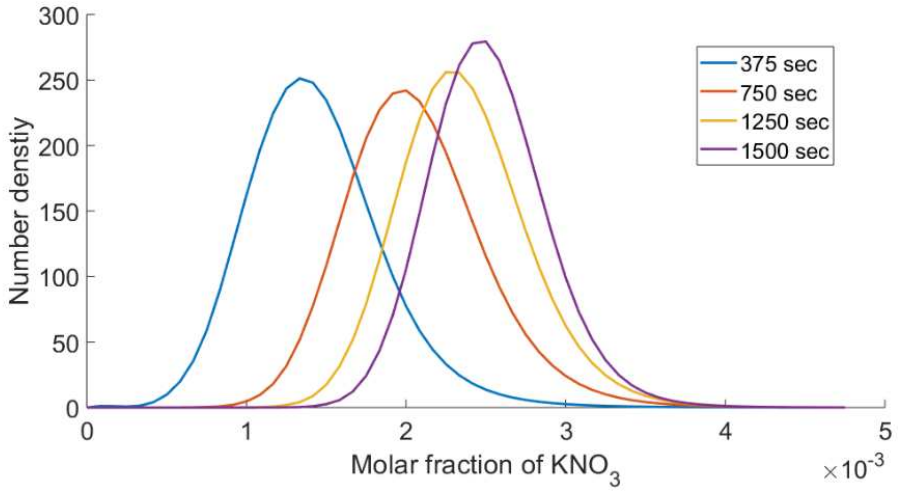

Fig. 6 Time-dependent crystal KNO_3 concentration distribution

Another simulation was carried out for $NaNO_3$ crystallization without KNO_3 impurities. Except the initial amount of KNO_3 in solution, all other initial conditions are the same as the case above. The comparison of facet normal distance distributions are shown in Fig. 7. The increasing rate of normal distances of {104} face in the case with KNO_3 (solid curve in the first figure) is significantly smaller than that in the case without KNO_3 (dash curve in the first figure) because KNO_3 poisoned the growth of {104} face. On the other hand the normal distances of the other two faces of the two cases are very similar under the assumption that the impurity doesn't affect these two faces and the parameters corresponding to KNO_3 on these two faces are assigned as 0.

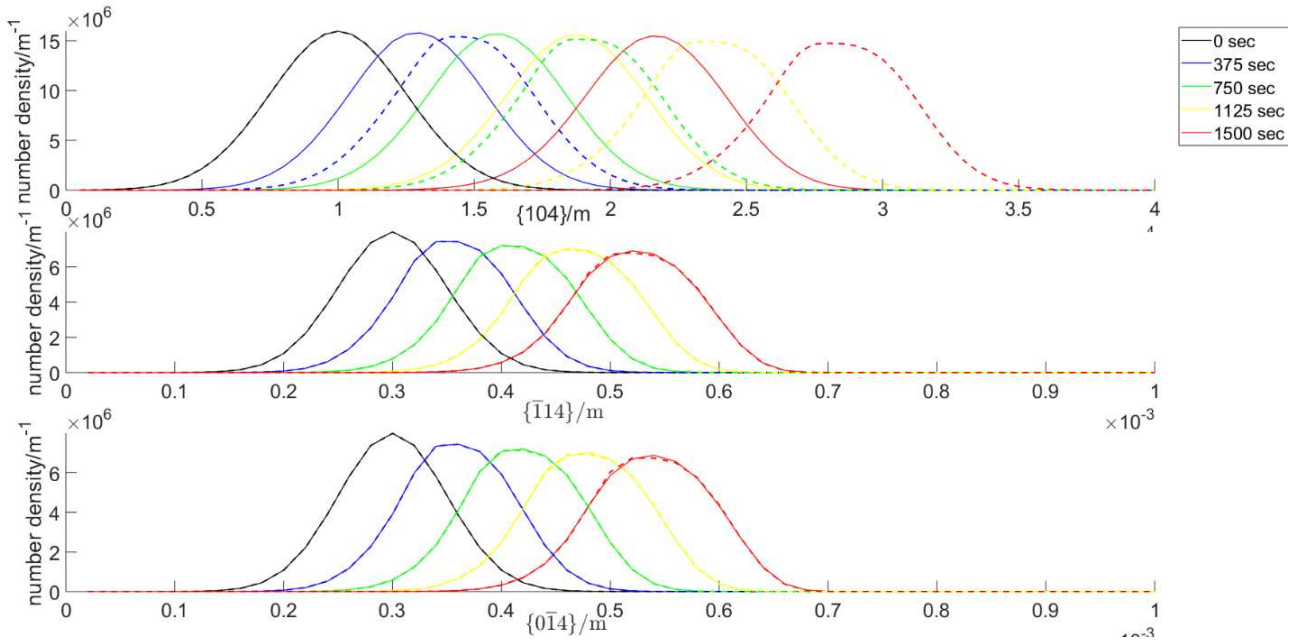

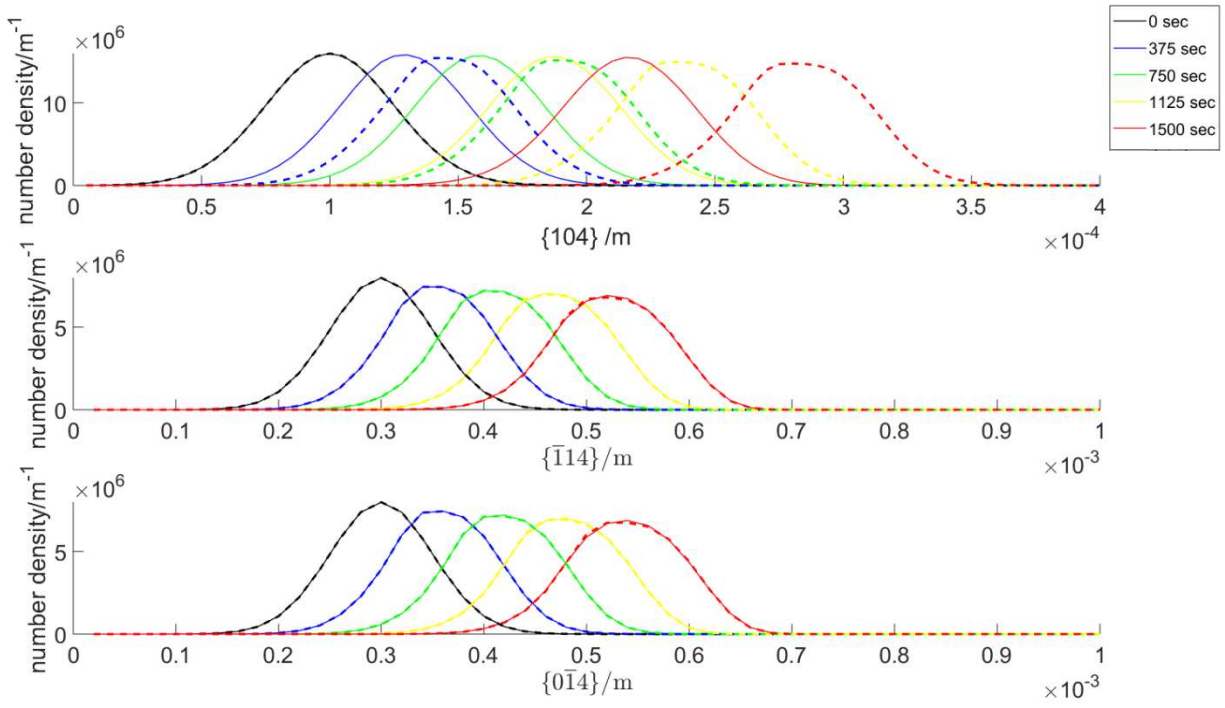

Fig. 7 Comparison of facet normal distance distribution of crystallization with and without KNO_3: Different colors represents different moments. Solid curves represent crystallization with KNO_3 impurities and Dash curves represent crystallization without KNO_3 impurities

Further Discussion

M^3PBEs provide unprecedented modeling capability fully based on first principle equations. The model parameter values can be obtained via three approaches: direct experimental measurement using instrument, estimation using molecular simulation (for some parameters), as well as model identification using data from crystallization experiments and an optimization approach together with the M3PBEs model.

The most reliable approach is direct experimental measurement using instrument. For instance, $k^d_{i,k}$, the liquid phase mass transfer coefficient can be measured by solid dissolution[16]. There are also correlations available for its estimation like the correlation given by Geankoplis, which can be used to predict the mass-transfer coefficients from liquid phase to the surface of small catalyst particles, microorganisms and other solids or liquid drops[12]. Solubility data could be used to estimate mass transfer coefficients, for

instance, $K_{i,k}$ (Langmuir constant of adsorption) and $K^r_{i,k}$ (the equilibrium ratios) were correlated with the solubility data; if $K_{i,k}$ can be obtained, $K^r_{i,k}$ can be calculated using the correlation relations.[1]

For some parameters, currently they may not be easily measured in experiments, but molecular simulation could be an alternative approach to estimate their values. For example, the parameters corresponding to mass transfer from adsorption layer to solid phase, $k^r_{i,k}$ (the mass transfer coefficient from adsorbed solute to crystallized solute) and r (the reaction order) canbe calculated with molecular simulation.

A not so rigorous but nevertheless practical method for estimation of parameter values is via model identification. Data from crystallization experiments and analysis of crystal shape and composition can be used, together with an optimization method to estimate the parameter values.

It should be noted that there may be errors in measurements or estimation of the parameter values. Therefore a sensitivity of parameters was discussed in the previous work[1]. The focus of the current paper is on building the M^3PBE modeling framework, future research could include developing new instrument and methods for accurate measurement and estimation of parameter values.

Future work should also consider the integration of M^3PBE with computational fluid dynamics in order to model large scale industrial processes, as well as more effective numerical solutions methods that can reduce the solution time of equations.

Conclusion

The proposed multi-stage multi-component transfer rate morphological population balance equations (M^3PBEs) enable the temporal and spatial distribution of multiple components inside individual crystals of a population in a crystallizer, as well as crystal shape and multi-dimensional size distributions to be modeled. The potential use of the new modeling technique in estimation of a drug's stability, modeling co-crystallization of two or multiple components, as well as in dealing with other challenging crystallization processes such as chiral drug separation via

crystallization is open for future exploration. Future research should also investigate M^3PBEs integration with computational fluid dynamics for use in large scale crystallizers, new instrument and methods for parameter measurement and estimation, as well as more efficient mathematical algorithms for solution of M^3PBEs equations.

Acknowledgements

Financial support from the National Natural Science Foundation of China (NNSFC) (grant references: 61633006, 91434126, 21706075), the Natural Science Foundation of Guangdong Province (grant reference: 2014A030313228), the Guangdong Provincial Science and Technology Projects under the Scheme of Applied Science and Technology Research Special Funds (grant reference: 2015B020232007), as well as China Postdoctoral Science Foundation (Grant No. 2016M592491) is acknowledged. The authors would like to extend their gratitude to the anonymous reviewers whose constructive comments greatly helped improvement of the article.

References

1. Shu, Y. D.; Li, Y.; Zhang, Y.; Liu, J. J.; Wang, X. Z. A multi-component mass transfer rate based model for simulation of non-equilibrium growth of crystals. *CrystEngComm* **2018,** *20* (35), 5143-5153.
2. (a) Kubota, N.; Mullin, J. W. A kinetic model for crystal growth from aqueous solution in the presence of impurity. *Journal of Crystal Growth* **1995,** *152* (3), 203-208; (b) Kubota, N. Effect of impurities on the growth kinetics of crystals. *Crystal Research and Technology* **2001,** *36* (8-10), 749-769; (c) Kubota, N.; Sasaki, S.; Doki, N.; Minamikawa, N.; Yokota, M. Adsorption of an Al (III) impurity onto the (100) face of a growing KDP crystal in supersaturated solution. *Crystal Growth & Design* **2004,** *4* (3), 533-537.
3. Borsos, A.; Majumder, A.; Nagy, Z. K. Multi-Impurity Adsorption Model for Modeling Crystal Purity and Shape Evolution during Crystallization Processes in Impure Media. *Crystal Growth & Design* **2016,** *16* (2), 555-568.
4. Ma, C. Y.; Wang, X. Z.; Roberts, K. J. Morphological population balance for modeling crystal growth in face directions. *Aiche Journal* **2008,** *54* (1), 209-222.
5. Karpiński, P. H. Importance of the two-step crystal growth model. *Chemical Engineering Science* **1985,** *40* (4), 641-646.
6. Martins, P. M.; Rocha, F. A new theoretical approach to model crystal growth from solution. *Chemical Engineering Science* **2006,** *61* (17), 5696-5703.
7. Krishnamurthy, R.; Taylor, R. A nonequilibrium stage model of multicomponent separation processes. Part I: Model description and method of solution. **1985,** *31* (3), 449- 456.
8. Gunawan, R.; Fusman, I.; Braatz, R. D. High resolution algorithms for multidimensional population balance equations. *Aiche Journal* **2004,** *50* (11), 2738-2749.

9. Benages-Vilau, R. Growth, Morphology and Solid State Miscibility of Alkali Nitrates. Universitat de Barcelona, 2013.

10. Wu, K.; Ma, C. Y.; Liu, J. J.; Zhang, Y.; Wang, X. Z. Measurement of Crystal Face Specific Growth Kinetics. *Crystal Growth & Design* **2016,** *16* (9), 4855-4868.

11. Benages-Vilau, R.; Calvet, T.; Pastero, L.; Aquilano, D.; Angel Cuevas-Diarte, M. Morphology Change of Nitratine (NaNO3) from Aqueous Solution, in the Presence of Li+ and K+ Ions. *Crystal Growth & Design* **2015,** *15* (11), 5338-5344.

12. Geankoplis, C. J. *Transport processes and unit operations*. Allyn & Bacon: 1978; p x+650.

13. Graber, T. A.; Taboada, M. E.; Alvarez, M. N.; Schmidt, E. H. Determination of mass transfer coefficients for crystal growth of nitrate salts. *Crystal Research and Technology* **1999,** *34* (10), 1269-1277.

14. Xu, T.; Pruess, K. Thermophysical properties of sodium nitrate and sodium chloride solutions and their effects on fluid flow in unsaturated media. *Office of Scientific & Technical Information Technical Reports* **2001**.

15. Rolfs, J.; Lacmann, R.; Kipp, S. Crystallization of potassium nitrate (KNO3) in aqueous solution .1. Growth kinetics of the pure system. *Journal of Crystal Growth* **1997,** *171* (1-2), 174-182.

16. Pitault, I.; Fongarland, P.; Koepke, D.; Mitrovic, M.; Ronze, D.; Forissier, M. Gas–liquid and liquid–solid mass transfers in two types of stationary catalytic basket laboratory reactor. *Chemical Engineering Science* **2005,** *60* (22), 6240-6253.